Reactor antineutrino spectra and their application to antineutrino-induced reactions

B. R. Davis and P. Vogel
California Institute of Technology, Pasadena, California 91125

F. M. Mann and R. E. Schenter
Hanford Engineering Development Laboratory, Richland, Washington 99352

(Received 13 December 1978)

The knowledge of reactor antineutrino spectra is necessary for the interpretation of weak-interaction experiments located at nuclear reactors. We calculate the antineutrino and electron spectra accompanying thermal neutron fission of ^{235}U and ^{239}Pu for various irradiation times. It is stressed that the higher energy part ($E \gtrsim 4$ MeV) of the spectra depends sensitively on the β-decay characteristics of fission products with experimentally unknown decay schemes. We also discuss the accuracy of a semiempirical conversion of the electron spectrum into the antineutrino spectrum. The resulting $\bar{\nu}_e$ spectra are used to calculate cross sections and reaction rates for the inverse neutron β decay, weak charged and neutral current induced deuteron disintegration, and the antineutrino-electron scattering.

[RADIOACTIVITY, FISSION ^{235}U, ^{239}Pu; Antineutrino and electron spectra calculated. σ for $\bar{\nu}$ induced reactions analyzed.]

I. INTRODUCTION

Valuable information about the structure of weak neutral and charged currents can be derived from the study of neutrino-induced reactions. These reactions may be also used as a source of information about the fundamental properties of the neutrino,[1] such as possible neutrino oscillations. Nuclear reactors, as sources of electron antineutrinos, give fluxes of the order $\sim 10^{13}$ $\bar{\nu}/\mathrm{cm}^2$ sec at distances ~ 10 m from the reactor core. These antineutrinos have an energy spectrum peaked at very low energies (~ 0.3 MeV) and extending up to ~ 10 MeV, characteristic of the β^- decay of the fission products.

Table I lists the antineutrino-induced reactions studied at nuclear reactors. Three of the reactions listed in the Table were actually observed. The first one, the inverse β decay of the neutron, was observed in the pioneering work of Reines and his collaborators. The most recent measurement of the total cross section[2] has an accuracy of 15%. The charged current deuteron disintegration was observed by Jenkins *et al.*[3] with $\sim 50\%$ accuracy, and $\bar{\nu}$-electron scattering was recently observed by Reines *et al.*[4] with 25% accuracy. All four reactions listed in the Table are currently being studied again in a new generation of experiments, and more detailed information is expected. For example, it seems feasible to determine not only the total cross section of the inverse neutron β decay, but also the positron spectrum with accuracy better than 10%.

TABLE I. Reactor antineutrino-induced reactions.

Reaction	σ_{tot} in 10^{-44} cm^2/fission [a]	Threshold in MeV
$\bar{\nu}+p \rightarrow n+e^+$	60	1.8
$\bar{\nu}+d \rightarrow n+n+e^+$	1.2	4.0
$\bar{\nu}+d \rightarrow n+p+\bar{\nu}$	2.9	2.3
$\bar{\nu}+e^- \rightarrow \bar{\nu}+e^-$.	0.4 [b]	1.7 [c]

[a] Based on our present calculation of the antineutrino spectrum for 30 days exposure time.
[b] For the Weinberg-Salam theory with $\sin^2\theta_W = 0.25$.
[c] This is a "practical" threshold assuming that electrons with kinetic energy below 1.5 MeV are impossible to observe.

In order to make useful conclusions about the underlying fundamental weak interactions, one has to know the spectrum of antineutrinos impinging on the target, with accuracy comparable to, or better than, the accuracy of the measured cross sections. Thus a considerable effort was devoted in the past to the problem of determining the antineutrino spectra.

There are basically two methods of approach. The first one, developed in Refs. 5 and 6, uses the experimentally determined electron spectrum and converts it into the antineutrino spectrum. We shall discuss this method in greater detail in Sec. III. The second method is seemingly the obvious one. A catalog of all fission fragments and their yields is made, including all the β-decay branches. Using the allowed Coulomb corrected spectral shape, one adds the contributions of all of them. Such a calculation was first performed by Perkins and King.[7] Later calculations, with more complete experimental data, were reported by Avignone and his collaborators, Refs. 8–10, and by Borovoi, Dobrynin, and Kopeikin.[11] The main problem, as will be seen below, is insuffi-

cient knowledge of β-decay schemes of fission fragments with large Q values and correspondingly short lifetimes.

In this work we report the results of our calculations of antineutrino spectra and their application to the interpretation of antineutrino-induced reactions. Our results differ substantially from those of Refs. 9–11. We also believe that the previously reported theoretical uncertainties[9] are too optimistic, and we attempt to estimate these uncertainties in a more realistic way. Preliminary results of our work were reported earlier.[12]

While our calculations were in progress, we learned that another group, Rudstam and Aleklett,[13] also calculated the reactor antineutrino spectra. Their conclusions are quite similar to ours; in particular, they predict fewer high energy antineutrinos than Refs. 9–11.

In the past it was customary to normalize the calculated spectra and cross sections per fission antineutrino. However, while the number of fissioning nuclei per second is usually accurately known, the total number of antineutrinos is much more uncertain. Moreover, as seen in Table I, only the approximately 30% of $\bar{\nu}$'s with energies above ~2 MeV are relevant for our purpose. Thus, in the following we report all our results "per fission" and avoid the largely misleading normalization "per antineutrino."

II. CALCULATION OF THE SPECTRA

The antineutrino spectrum is given by

$$N(E_{\bar{\nu}}) = \sum_n Y_n(Z,A,t) \sum_i b_{n,i}(E_0^i) P(E_{\bar{\nu}}, E_0^i, Z) . \tag{1}$$

Here $Y_n(Z,A,t)$ is the "effective" cumulative fission yield of the nucleus Z,A (possibly isomeric state) after exposure time t. In our calculation we have used the thermal neutron fission yields of the nuclear data file ENDF/B-V (Evaluated Nuclear Data File version V).[14] The effect of delayed neutrons was included explicitly. The transmutations of fission fragments by reactor neutrons was also included; a neutron flux of $3\times 10^{13} n/\mathrm{cm}^2$ sec was assumed. The fission yields of the nuclei with large Q values are almost independent of this effect.

The quantities $b_{n,i}(E_0^i)$ in Eq. (1) are branching ratios for the ith branch with the maximal electron energy $E_0^i = Q_n + m_e c^2 - E_{\mathrm{exc}}^i$, where Q_n is the Q value of the species n, and E_{exc}^i is the excitation energy in the daughter nucleus. They are normalized such that $\sum_i b_{n,i}(E_0^i) = 1$, except for isomeric states, where the sum is smaller than one due to the γ decay.

We assume that all branches have the allowed spectral shape, i.e.,

$$P(E_{\bar{\nu}}, E_0, Z) = k E_{\bar{\nu}}^2 (E_0 - E_{\bar{\nu}})^2 G(E_0 - E_{\bar{\nu}}, Z) , \tag{2}$$

where P is normalized to unity (k is the normalization constant). The function G in Eq. (2) is related to the usual Fermi Coulomb function. It depends on Z and on the total electron energy $E_\beta = E_0 - E_{\bar{\nu}}$ (P_β is the electron momentum):

$$G(E_\beta, Z) \equiv P_\beta / E_\beta F(E_\beta, Z) . \tag{3}$$

In our calculation we usually use a simple analytic approximation to G which agrees to within ~5% with the corresponding exact expression.

We used the β-decay data of ENDF/B-IV.[14] This file contains 710 fission products (including isomers), of which about 200 have complete experimentally determined decay schemes. The remaining ("unknown") were treated in the following way:

(a) The Q values were checked and replaced by new experimental or systematic data whenever appropriate.

(b) For ~60 nuclei the continuous β-feed distributions of Aleklett *et al.*[15] were used. These additional nuclei contribute ~20% of the neutrino spectrum for energies above 4 MeV.

(c) For the remaining nuclei, out of which ~80 have large enough yields and Q values to contribute significantly to $\bar{\nu}$ spectra above 4 MeV, various prescriptions were used, as described below.

In the past, a simple two-branch formula[8,11] was used for the nuclei with unknown branchings. It was assumed that there are no branches to levels above the pairing energy in the daughter nucleus (except for the odd-odd daughter nuclei). Such a prescription probably overestimates the actual branching with large end point energies, as demonstrated by the experimental results of Ref. 15.

Thus we adopted the assumption[15] that the average reduced transition rate is constant, independent of the excitation energy in the daughter nucleus. This leads to the following expression for the β-feeding probability:

$$b(E_0) = k' \rho(Q + m_e c^2 - E_0) f(E_0, Z+1) , \tag{4}$$

where k' is the normalization, $\rho(E_{\mathrm{exc}})$ is the nuclear level density, and $f(E_0, Z+1)$ is given by (note that Z is the parent nucleus charge)

$$f(E_0, Z+1) = \int_{m_e c^2}^{E_0} E_\beta^2 (E_0 - E_\beta)^2 \times G(E_\beta, Z+1) dE_\beta . \tag{5}$$

For the nuclear level density we used the formula of Ref. 15 and the parameters of Ref. 16, evaluated for $I = 1$ as a typical spin value. The final result is only weakly dependent on this assumption (the spectrum changes by at most 1% when $I = 1$ is replaced by $I = 3$). Formula (4) is used for excitation energies above the pairing energy P and the $b(E_0)$ for these energies are normalized to

$$\sum_{E_{\text{exc}}>P} b(E_0) = \alpha' \ . \tag{6}$$

The values of α' were found by averaging the results of Ref. 15. We use $\alpha' = 1$ for odd-odd daughters, $\alpha' = 0.53$ for nuclei with $Q - P \geq 5$ MeV and $A < 110$, $\alpha' = 0.36$ for $Q - P \geq 5$ MeV and $A > 110$, and $\alpha' = 0.28$ for the remaining nuclei. The remaining branching $1 - \alpha'$ was equally distributed among three hypothetical states with energies 0, $P/3$, $2P/3$.

That the average reduced transition rate is approximately constant is an empirical fact which follows from the study[15] of neutron-rich fission products with large Q values, i.e., the nuclei similar to the "unknown" set. Two opposing influences affect the transition rate. The level density used in Eq. (4) is an overestimate, because only states obeying the quasiparticle selection rules contribute to β decay. On the other hand, one expects an increase of transition rate with excitation energy as unhindered configurations, or the giant Gamow-Teller resonance, become populated. It is our belief that the just described prescription for estimating the unknown branching ratios is more realistic than those used before in the literature.

Examples of the calculated antineutrino and electron spectra are shown in Tables II and III. Columns 2–4 in both Tables are based on the present prescription for treatment of the unknown decay schemes. They illustrate the dependence of the spectrum on the exposure time. Note that at higher energies ($E \geq 3$ MeV) the spectra are essentially independent of the exposure time. Indeed, the high-energy electrons and $\bar{\nu}$'s come from the β decay of fission fragments with large Q values and correspondingly short lifetimes. Such nuclei reach equilibrium in a short time, and their fission yields in Eq. (1) are simply the corresponding cumulative yields.

Columns 5 and 6 in both Tables illustrate the sensitivity of the results to the prescription used for treatment of unknown nuclei. In particular, column 6 shows the upper bound spectrum, where we assumed (unrealistically) that all unknown nuclei decay directly to the ground state. The results in column 5 were obtained using our data file together with the two-branch prescription of Ref. 8. The differences between these results and Ref. 8 are apparently caused by the differences in input data. In particular, we include as "known" the nuclei studied in Ref. 15.

The last columns in Tables II and III show the $\bar{\nu}_e$ and electron spectra corresponding to the thermal neutron fission of ^{239}Pu. As noted earlier[10,11] such spectra are considerably softer. Thus, for practical applications it is very important to know the relative amount of ^{235}U and ^{239}Pu fission for each particular experiment.

In column 7 of Table II we show the latest results of Avignone and Hopkins.[10] Their spectrum contains considerably more high energy $\bar{\nu}_e$'s than in any other similar calculation.

The electron spectra accompanying fission may be directly measured. However, only a few accurate measurements were performed for "zero

TABLE II. Antineutrino spectra.

Energy	^{235}U exposure time			Avignone	Ground state	Avignone	^{239}Pu
MeV	3 hours [a]	30 days [a]	3 years [a]	prescription [b]	prescription [c]	Purdue [d]	7 days exposure [a]
1.0	1.56	2.23	2.38	2.12	2.10	...	2.07
1.5	1.35	1.56	1.65	1.55	1.53	1.64	1.34
2.0	1.05	1.16	1.21	1.18	1.18	1.33	9.82(−1)
2.5	7.66(−1)	8.19(−1)	8.42(−1)	8.51(−1)	8.61(−1)	...	6.81(−1)
3.0	5.72(−1)	5.93(−1)	5.95(−1)	6.33(−1)	6.44(−1)	7.41(−1)	4.88(−1)
4.0	2.69(−1)	2.73(−1)	2.73(−1)	2.96(−1)	3.19(−1)	3.58(−1)	2.03(−1)
5.0	1.02(−1)	1.03(−1)	1.03(−1)	1.12(−1)	1.37(−1)	1.37(−1)	6.77(−2)
6.0	3.50(−2)	3.50(−2)	3.50(−2)	4.14(−2)	5.25(−2)	5.73(−2)	2.08(−2)
7.0	1.01(−2)	1.01(−2)	1.01(−2)	1.27(−2)	1.74(−2)	1.94(−2)	5.03(−3)
8.0	1.87(−3)	1.87(−3)	1.87(−3)	2.78(−3)	4.91(−3)	5.85(−3)	8.14(−4)

[a] Present prescription for unknown decays (see text).
[b] 30 days exposure time, unknown decays treated with the two-branch prescription of Ref. 8.
[c] 30 days exposure time, nuclei with unknown decays allowed to decay only to the daughter ground state.
[d] Calculated spectrum of Ref. 10.

TABLE III. Electron spectra.

Total energy MeV	^{235}U exposure time 3 hours [a]	30 days [a]	3 years [a]	Avignone prescription [b]	Ground state prescription [c]	Univ. of Illinois exp. [d]	^{239}Pu 7 days exposure [a]
1.0	1.93	2.87	2.99	2.75	2.72	2.72	2.65
1.5	1.49	1.81	1.92	1.78	1.76	2.09	1.57
2.0	1.10	1.23	1.28	1.24	1.24	1.37	1.04
2.5	7.85(−1)	8.43(−1)	8.67(−1)	8.78(−1)	8.84(−1)	9.10(−1)	7.03(−1)
3.0	5.62(−1)	5.87(−1)	5.95(−1)	6.24(−1)	6.36(−1)	6.08(−1)	4.79(−1)
4.0	2.52(−1)	2.56(−1)	2.56(−1)	2.78(−1)	3.00(−1)	2.73(−1)	1.89(−1)
5.0	9.36(−2)	9.46(−2)	9.46(−2)	1.04(−1)	1.26(−1)	1.06(−1)	6.17(−2)
6.0	3.18(−2)	3.18(−2)	3.18(−2)	3.75(−2)	4.74(−2)	3.95(−2)	1.89(−2)
7.0	9.04(−3)	9.04(−3)	9.04(−3)	1.14(−2)	1.54(−2)	1.35(−2)	4.56(−3)
8.0	1.71(−3)	1.71(−3)	1.71(−3)	2.50(−3)	4.40(−3)	4.00(−3)	7.57(−4)

[a] Present prescription for unknown decays (see text).
[b] 30 days exposure time, unknown decays treated with the two-branch prescription of Ref. 8.
[c] 30 days exposure time, nuclei with unknown decays allowed to decay only to the daughter ground state.
[d] Experimental spectrum of Ref. 17, 3 hours exposure time.

cooling time" relevant for our calculations. Column 7 of Table III shows an example of such a spectrum measured by Tsoulfanidis *et al.*[17] Our calculated spectrum for the same three hour exposure time does not agree very well with the data, particularly at lower energies ($E \leq 2$ MeV). Actually, we verified that at these low energies our calculations predict ~30% fewer electrons at all exposure times $t \leq 8$ hours, independent of the prescription used for the unknown nuclei. The situation is better at higher energies, which are more relevant for the antineutrino reactions. For $2 < E \leq 6$ MeV the calculated spectrum using our prescription (column 2, Table III) is only ~10% below the data.[17] We can only speculate about the source of the low energy discrepancy. Let us note, however, that the experimental electron spectra were actually determined in two separate experiments. The low energy data come directly from Ref. 17, while the high energy electrons were measured earlier[18] and reanalyzed. It seems that the earlier spectra of Ref. 18 contain fewer electrons than the corresponding numbers in Tables I and II of Ref. 17. The discrepancy between the exposure time dependence of the low energy electron spectra calculated by us and measured in Refs. 17 and 18 stresses the need of new accurate measurements.

There are various sources of uncertainty in the resulting spectra. One possible source of error is the actual experimental error in branchings for known nuclei, and in the fission yields and Q values of all nuclei. Another source of error is associated with the experimental continuous β-feed distributions of Aleklett *et al.*[15] We did not attempt to include these uncertainties in our analysis, but we estimated that the corresponding error is about 10% and that it does not vary substantially with the neutrino (electron) energy. In our judgment the major uncertainty is related to the value α' [Eq. (6)] characterizing the β feeding above the pairing energy. Figure 1 illustrates the corresponding spread of the resulting spectrum. The error in α' was estimated from the width of the α' distribution of nuclei studied in Ref. 15. Thus we used 40% uncertainty in α' for $Q - P > 5$ MeV and 80% uncertainty in α' for $Q - P < 5$ MeV.

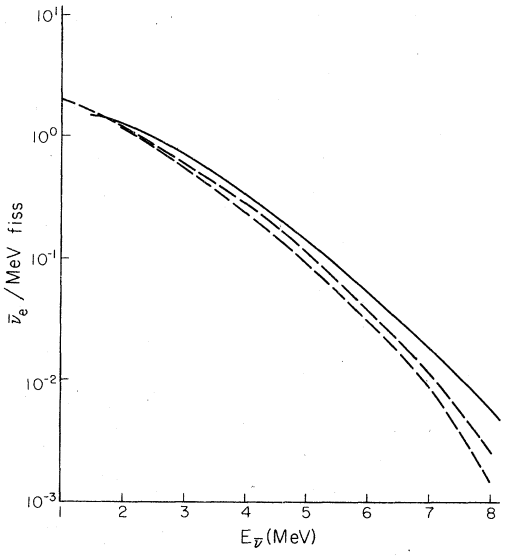

FIG. 1. Upper and lower limits of the present calculated antineutrino spectrum (dashed curves)—see text for explanation. The full curve shows, for comparison, the spectrum calculated in Ref. 10.

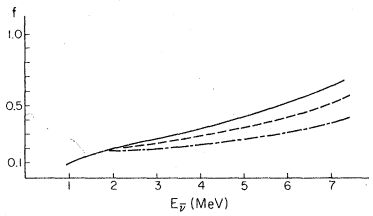

FIG. 2. The relative role of "unknown" nuclei at various antineutrino energies. "f" is the fraction of the antineutrinos emitted from nuclei with unknown decay schemes. The full curve corresponds to the ground state decay of unknown nuclei; the dashed curve was calculated with the two-branch formula of Ref. 8; dot and dashed curve calculated with the present prescription, Eq. (4).

Figure 1 also shows how far the spectrum of Avignone and Hopkins[10] is from our present calculation.

Figure 2 illustrates the crucial role played by the unknown nuclei. These nuclei contribute relatively little to the integral quantities, such as the total number of electrons (or $\bar{\nu}_e$), the total electron energy, and the total fission yield. Their contribution to the high energy tail of the spectrum is, however, greatly enhanced. This crucial role of the unknown nuclei was not sufficiently stressed in previous studies of the problem.[8-11]

The actual form of the theoretical β-feed function $b(E_0)$ [Eq. (4)] is illustrated in Fig. 3 and compared with experiment.[15] The agreement in this particular case is excellent. The qualitative features of $b(E_0)$ are similar in all nuclei. They are related to the fast increase of the nuclear level density $\rho(E_{\rm exc})$, which competes with the fast decreasing $\sim(Q+m_ec^2-E_{\rm exc})^5$ spectral shape factor. Our results are relatively insensitive to the distribution of the $1-\alpha'$ feeding among the states below the pairing energy P.

III. RELATION BETWEEN REACTOR ELECTRON AND ANTINEUTRINO SPECTRA

In the β^- decay of a fission product with a given Q value two particles are emitted: an electron of total energy $E_\beta = Q + m_ec^2 - E_{\bar{\nu}}$ and an antineutrino with energy $E_{\bar{\nu}}$. Obviously, both spectra are determined by the same function $n(Z, E = Q + m_ec^2)$ which describes the distribution of end points in Z and E. The question arises whether, given an experimentally measured electron spectrum, one can infer the function $n(Z, E)$ and determine the antineutrino spectrum. It was our objective to study quantitatively the accuracy of this method, first proposed by Muelhause and Oleksa,[5] and further developed by Carter *et al.*[6]

Following Ref. 6 we shall neglect the Z dependence of $n(Z, E)$ and assume that the number of electrons per MeV is equal to

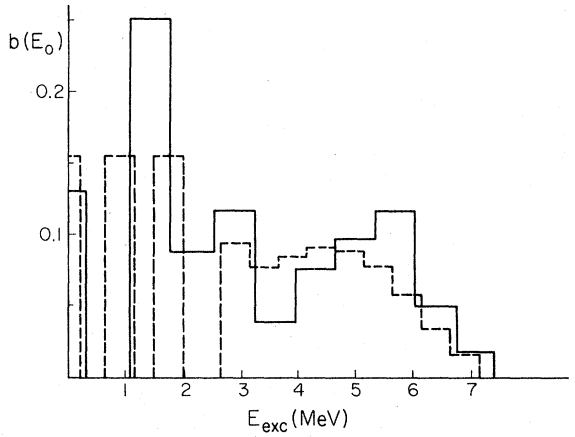

FIG. 3. β feeding for the decay of ^{86}Br, $Q = 8.0$ MeV. The full histogram shows experimental data of Ref. 15 and the dotted histogram shows the calculated results using Eq. (4).

$$Y(E_\beta) = \int_{E_\beta}^{\infty} dE\, n(Z, E) k(Z, E) E_\beta^2 (E - E_\beta)^2 G(E_\beta, Z), \tag{7}$$

where $k(Z, E)$ is the normalization for the allowed spectrum. The end point distribution $n(Z, E)$ is then equal to

$$n(Z, E) = -\frac{1}{2k(Z, E)} \frac{d^3}{dE^3} \left(\frac{Y(E)}{E^2 G(E, Z)} \right). \tag{8}$$

An example of the resulting end point distribution $n(Z, E)$ is shown in Fig. 4 for two extreme values of Z. We see that this function is practically independent of Z, thus giving *a posteriori* justifica-

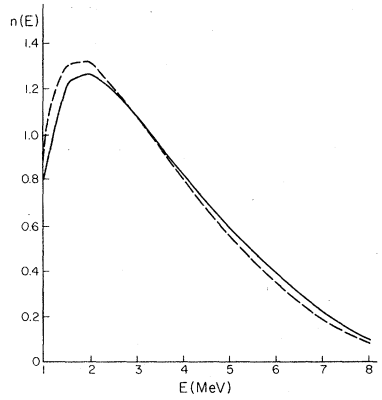

FIG. 4. The end point energy distribution function $n(Z, E)$, Eq. (8) in arbitrary units. The full curve is calculated for $Z = 60$, the dashed curve for $Z = 32$. As input the electron spectrum of ^{235}U in column 4, Table III, is used.

tion of Eq. (7). We have verified that the function $n(Z,E)$ depends only slightly on Z in all the cases we studied.

Thus it appears that we have arrived at a "universal" end point distribution function, which can now be applied to generate the reactor antineutrino spectrum

$$X(Z,E_{\bar{\nu}}) = \int_{E_{\bar{\nu}}+m_e c^2}^{\infty} dE\, n(Z,E) k(Z,E) \times E_{\bar{\nu}}^2 (E-E_{\bar{\nu}})^2 G(E-E_{\bar{\nu}},Z). \quad (9)$$

Since the ^{235}U fission products are distributed in two peaks at low and high mass regions, it seems reasonable to express the reactor $\bar{\nu}_e$ spectrum as the average of the two spectra evaluated at the mean charge of each peak. The final antineutrino spectrum depends only slightly on the actual prescription for this averaging, as long as both peaks in the fission fragment distribution are included with equal weight.

We tested quantitatively the accuracy of the above procedure for various electron spectral shapes $Y(E_\beta)$. This was done by generating both the electron and antineutrino spectra using the program described in Sec. II, and then converting the electron spectrum into the antineutrino spectrum. We find that the conversion program has accuracy of better than 10% at each energy up to ~7.5 MeV for typical electron spectra. This is illustrated in Fig. 5, where the relative error of conversion is plotted:

$$\Delta = \frac{N_{\rm conv}(E_{\bar{\nu}}) - N_{\rm gener}(E_{\bar{\nu}})}{N_{\rm gener}(E_{\bar{\nu}})}. \quad (10)$$

Such a conversion method, together with an accurate experimental e^- spectrum, may be a valuable tool in the attempt to derive a correct $\bar{\nu}_e$ spectrum.

IV. APPLICATION TO ANTINEUTRINO-INDUCED REACTIONS

In this Section we apply the resultant antineutrino spectrum to the calculation of the corresponding reaction rates. We discuss in more detail the four antineutrino-induced reactions listed in Table I. To stress the sensitivity of the results to the shape and magnitude of the reactor antineutrino spectrum, we compare our present results with the most recent calculations of Ref. 10. We do not show the "theoretical error" in our plots. One should remember, however, that we estimate a theoretical uncertainty gradually increasing from ~10% at $E_{\bar{\nu}}=2$ MeV to ~30% at $E_{\bar{\nu}}=8$ MeV.

The inverse neutron β decay $\bar{\nu}_e + p \rightarrow n + e^+$ is the reaction with the largest cross section on our list. For monoenergetic antineutrinos the cross section is given by the expression

$$\sigma(E_{\bar{\nu}}) = 8.85\times10^{-44}[E_{\bar{\nu}} - (M_n - M_p)c^2] \times \{[E_{\bar{\nu}} - (M_n - M_p)c^2]^2 - (m_e c^2)^2\}^{1/2}\ \text{cm}^2, \quad (11)$$

where energies are measured in MeV and

$$8.85\times10^{-44}\ \text{cm/MeV}^2 = \frac{G^2}{\pi}(\hbar c)^2(f^2+3g^2),$$
$$g/f = 1.23, \quad G = \frac{1.0\times10^{-5}}{(M_p c^2)^2}. \quad (12)$$

Figure 6 shows the cross section for a given positron kinetic energy E_{e^+} (the small neutron recoil is neglected), that is (11) multiplied by the corresponding $\bar{\nu}_e$ spectrum. When integrated over all positron energies one obtains the total cross section in units of 10^{-44} cm^2/fission equal to 60 for the $\bar{\nu}_e$ spectrum calculated here and 80 for the $\bar{\nu}_e$ spectrum of Ref. 10. The experiment[2] gives 56 ± 8. This reaction is also of interest as a proposed detector of possible neutrino oscillations.[19,20]

The antineutrino electron scattering $\nu_e + e^- \rightarrow \nu_e + e^-$ is perhaps the most interesting on our list.

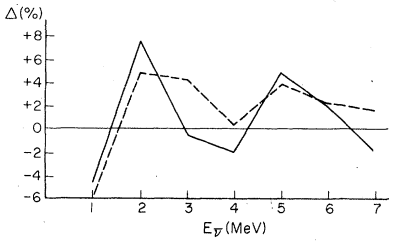

FIG. 5. The deviation Δ in percent, Eq. (14), for the ^{235}U fission (3 years exposure time)—full curve, and ^{239}Pu fission (7 days exposure time)—dashed curve.

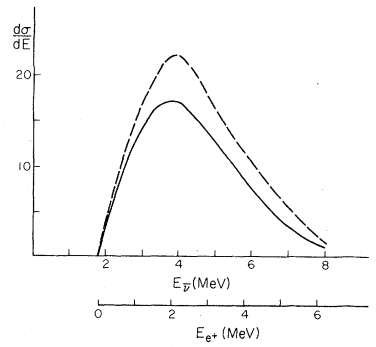

FIG. 6. Cross section for the reaction $\bar{\nu}+p \rightarrow n+e^+$ folded with the antineutrino spectrum, in 10^{-44} cm^2/MeV fission. The present spectrum was used to calculate the full curve, the spectrum of Ref. 10 was used in calculation of the dashed curve.

By measuring the differential cross section, i.e., the electron recoil spectrum, one can obtain valuable information about the structure of the weak interaction Hamiltonian. For monoenergetic $\bar{\nu}_e$'s and electron recoil kinetic energy T the cross section is given by the expression[4]

$$\frac{d\sigma(E_{\bar{\nu}})}{dT}=\frac{G^2 m_e c^2}{2\pi}(\hbar c)^2\left\{(C_V+C_A)^2+(C_V-C_A)^2\left(1-\frac{T}{E_{\bar{\nu}}}\right)^2+\frac{m_e c^2 T}{E_{\bar{\nu}}^2}(C_A{}^2-C_V{}^2)\right\}. \quad (13)$$

Here C_V (C_A) is the vector (axial vector) coupling constant. In the Weinberg-Salam theory one has $C_A=-\frac{1}{2}, C_V=\frac{1}{2}+2\sin^2\theta_W$. The observable electron spectrum is proportional to the cross section

$$\frac{d\sigma}{dT}=\int_{E_{\bar{\nu}}^{\min}}^{\infty}\frac{d\sigma(E_{\bar{\nu}})}{dT}N(E_{\bar{\nu}})dE_{\bar{\nu}}, \quad (14)$$

where $E_{\bar{\nu}}^{\min}$ is the minimum antineutrino energy allowed by kinematics. In practice, the antineutrinos in the vicinity of minimal energy give the largest contribution to the integral (14). Figure 7 shows the cross section (14) integrated over an interval 1.5 MeV wide in the electron kinetic energy. Future accurate measurements of the recoil electrons in these energy intervals, combined with an accepted antineutrino spectrum, may constitute an effective test of the Weinberg-Salam theory in the leptonic sector.

The two deuteron-disintegration reactions have higher thresholds (2.23 MeV for the neutral current induced reaction, 4.03 MeV for the charged current reaction) than the inverse neutron β decay. This is one of the reasons for the corresponding cross sections being smaller. Another reason is the small overlap between the initial bound and final continuum state. Only the axial vector part of the weak current contributes to the deuteron disintegration at reactor antineutrino energies. In our calculation we use the cross section formulas of Ahrens and Lang.[21] The formulas were derived assuming a zero effective range of the nuclear forces. The meson exchange effects, known to contribute ~10% to the related n-p radiative capture, are also neglected. All of these approximations do not affect the main features of our results.

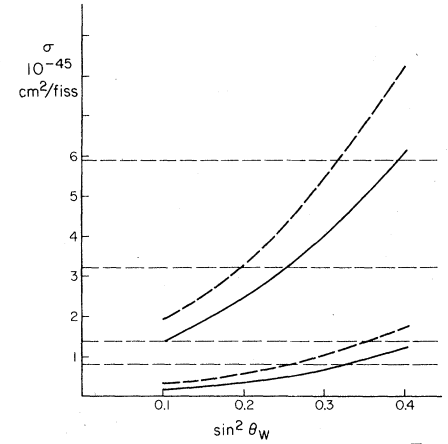

FIG. 7. The cross section for the reaction $\bar{\nu}+e^-\rightarrow\bar{\nu}+e^-$ as a function of the Weinberg angle θ_W. The lower set of curves corresponds to the integral over final electron kinetic energies $T=3-4.5$ MeV. The upper curves are for $T=1.5$—3 MeV. In each case the full line was calculated with the present $\bar{\nu}_e$ spectrum and the dashed line with the $\bar{\nu}_e$ spectrum of Ref. 10. The horizontal lines give the experimental limits of Ref. 4 recalculated "per fission."

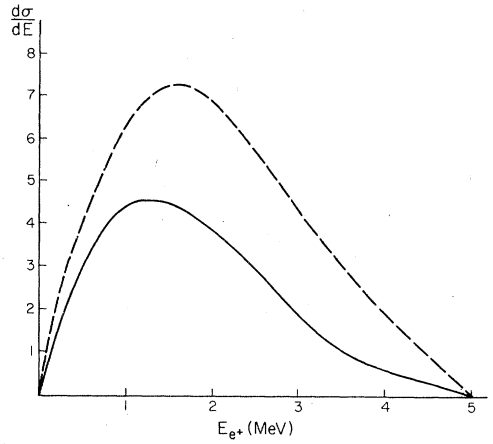

FIG. 8. The cross section of the reaction $\bar{\nu}+d\rightarrow n+n+e^+$ in 10^{-45} cm^2/MeV fission. See the notation of Fig. 6.

For the charged current reaction $\bar{\nu}+d\rightarrow n+n+e^+$ we show in Fig. 8 the predicted positron spectrum:

$$\frac{d\sigma}{dE_{e^+}}=\int_{E_{e^+}+E_T}^{\infty}\frac{d\sigma(E_{\bar{\nu}})}{dE_{e^+}}N(E_{\bar{\nu}})dE_{\bar{\nu}}, \quad (15)$$

where E_T is the reaction threshold. The total cross section in 10^{-44} cm^2/fission is equal to 1.2 for the present $\bar{\nu}_e$ spectrum and 2.1 for that of Ref. 10. The large difference between these two

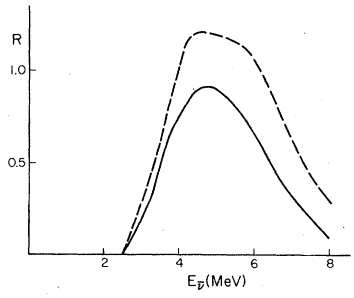

FIG. 9. The reaction rate $\sigma(E_{\bar{\nu}})N(E_{\bar{\nu}})$ for the reaction $\bar{\nu}+d\rightarrow n+p+\bar{\nu}$ in 10^{-45} cm^2/MeV fission. See the notation of Fig. 6.

cross sections is related to the threshold; the $\bar{\nu}_e$ spectra differ more at higher energies. The experimental cross section[3] is 1.8 ± 0.9.

For the neutral current deuteron disintegration $\bar{\nu} + d \rightarrow p + n + \bar{\nu}$ we show in Fig. 9 the reaction rate

$$R = \sigma(E_{\bar{\nu}}) N(E_{\bar{\nu}}) . \quad (16)$$

The total cross section in 10^{-44} cm^2/fission is equal to 2.9 for the present $\bar{\nu}_e$ spectrum and 4.3 for the $\bar{\nu}_e$ spectrum in Ref. 10. There are no experimental data on this reaction at the present time.

V. SUMMARY

We have verified that the high energy tail of the antineutrino and electron spectra depends sensitively on the treatment of nuclei with unknown β-decay schemes. The simple two-branch formula for such decays, used in previous calculations, considerably underestimates β branching to states above the pairing energy and, consequently, overestimates the number of high energy antineutrinos and electrons.

Besides using the most up-to-date experimental data available on known β-decay schemes, fission yields, nuclear masses, and Q values, we also include in our calculation the continuous β-feed results of Ref. 15. Thus our calculation reduces, to the greatest extent possible, the uncertainties present in the resulting spectra. Our treatment of the unknown nuclei is based on experimental studies of neutron-rich, high Q value nuclei, and would thus appear to be quite realistic.

We stress the potential importance of experimentally determined reactor electron spectra. An accurate spectrum can be compared with our results, testing our input data and prescription for unknown nuclei. It can also be used, in conjunction with the semiempirical conversion procedure discussed in Sec. III, to obtain the antineutrino spectrum directly.

The application of our calculation to antineutrino-induced reactions shows how sensitively the final measured cross sections depend on the input spectrum. Among the reactions we discussed, the situation is most critical in the case of the charged current deuteron disintegration, where the total cross section differs by a factor of 2 between our results and those of Ref. 10. On the other hand, the difference is considerably less (~30%) in the inverse neutron β decay and in the antineutrino electron scattering.

Note added in proof. The weak neutral and charged current deuteron disintegration was observed in the recent work by Pasierb *et al.* [Report No. UC Irvine 10P19-136 (unpublished)]. The measured cross sections, expressed as ratios to our predictions in Table I, are 0.8 ± 0.2 (neutral current) and 0.7 ± 0.2 (charged current).

We would like to thank Dr. Charles Reich for his help in preparing the input data and for numerous valuable discussions. We also benefited from discussions with Professor F. Boehm, Professor W. A. Fowler, and Professor V. Telegdi. One of the authors, P. V., would like to acknowledge the hospitality of the Aspen Center of Physics. This work was supported by DOE Grant Nos. EY-76-C-03-0063 and EY-76-C-14-2170 and NSF Grant No. PHY76-83685.

[1] S. M. Bilenky and B. Pontecorvo, Phys. Lett. 41C, 225 (1978), and references therein.
[2] F. A. Nezrick and F. Reines, Phys. Rev. 142, 852 (1966).
[3] T. L. Jenkins, F. E. Kinard, and F. Reines, Phys. Rev. 185, 1599 (1969).
[4] F. Reines, H S. Gurr, and H. W. Sobel, Phys. Rev. Lett. 37, 315 (1976).
[5] C. O. Muelhause and S. Oleksa, Phys. Rev. 105, 1332 (1957).
[6] R. E. Carter, F. Reines, J. J. Wagner, and M. E. Wyman, Phys. Rev. 113, 280 (1959).
[7] R. W. King and J. F. Perkins, Phys. Rev. 112, 963 (1958).
[8] F. T. Avignone III, Phys. Rev. D 2, 2609 (1970).
[9] F. T. Avignone III and Z. D. Greenwood, Phys. Rev. D 17, 154 (1978).
[10] F. T. Avignone III and L. P. Hopkins, in *Neutrinos*—78, Proceedings of the International Conference on Neutrino Physics and Astrophysics, Purdue, 1978, edited by E. C. Fowler (Purdue Univ. Press, Lafayette, Indiana, 1978), p. C42.
[11] A. A. Borovoĭ, Yu. L. Dobrynin, and V. I. Kopeĭkin, Yad. Fiz. 25, 264 (1977) [Sov. J. Nucl. Phys. 25, 144 (1977).
[12] B. R. Davis, P. Vogel, F. M. Mann, and R. E. Schenter, Bull. Am. Phys. Soc. 23, 927 (1978).
[13] G. Rudstam and K. Aleklett, Studsvik Sci. Res. Lab. report, 1978 (unpublished).
[14] Fission Product Decay Library of the Evaluated Nuclear Data File, Versions IV and V. Available from, and maintained by, the National Nuclear Data Center (NNDC) at the Brookhaven National Laboratory.
[15] K. Aleklett, G. Nyman, and G. Rudstam, Nucl. Phys. A246, 425 (1975).
[16] J. W. Truran, A. G. W. Cameron, and E. Hilf, CERN Report No. 70-30, 1970, Vol. 1, p. 275 (unpublished).
[17] N. Tsoulfanidis, B. W. Wehring, and M. E. Wyman, Nucl. Sci. Eng. 43, 42 (1971).
[18] J. W. Kutcher and M. E. Wyman, Nucl. Sci. Eng. 25, 435 (1966).
[19] F. Boehm, private communication and ILL annual report, Grenoble, 1977 (unpublished).
[20] F. Reines, in *Unification of Elementary Forces and Gauge Theories*, edited by D. B. Cline and F. E. Mills (Harwood, London, 1978), p. 103.
[21] T. Ahrens and T. P. Lang, Phys. Rev. C 3, 979 (1971).